Essential role of MALT1 protease activity in activated B cell-like diffuse large B-cell lymphoma

Stephan Hailfinger[a], Georg Lenz[b,1], Vu Ngo[b], Anita Posvitz-Fejfar[a], Fabien Rebeaud[a], Montserrat Guzzardi[a], Eva-Maria Murga Penas[c], Judith Dierlamm[c], Wing C. Chan[d], Louis M. Staudt[b], and Margot Thome[a,2]

[a]Department of Biochemistry, University of Lausanne, Chemin des Boveresses 155, CH-1066 Epalinges, Switzerland; [b]Metabolism Branch, Center for Cancer Research, National Cancer Institute, Bethesda, MD 20892; [c]Department of Oncology and Hematology, University Medical Center Hamburg-Eppendorf, Martinistrasse 52, D-20246 Hamburg, Germany; and [d]Department of Pathology and Microbiology, University of Nebraska, Omaha, NE 68198

Edited by Arthur Weiss, University of California, San Francisco, CA, and approved September 25, 2009 (received for review July 8, 2009)

A key element for the development of suitable anti-cancer drugs is the identification of cancer-specific enzymatic activities that can be therapeutically targeted. Mucosa-associated lymphoid tissue transformation protein 1 (MALT1) is a proto-oncogene that contributes to tumorigenesis in diffuse large B-cell lymphoma (DLBCL) of the activated B-cell (ABC) subtype, the least curable subtype of DLBCL. Recent data suggest that MALT1 has proteolytic activity, but it is unknown whether this activity is relevant for tumor growth. Here we report that MALT1 is constitutively active in DLBCL lines of the ABC but not the GCB subtype. Inhibition of the MALT1 proteolytic activity led to reduced expression of growth factors and apoptosis inhibitors, and specifically affected the growth and survival of ABC DLBCL lines. These results demonstrate a key role for the proteolytic activity of MALT1 in DLBCL of the ABC subtype, and provide a rationale for the development of pharmacological inhibitors of MALT1 in DLBCL therapy.

DLBCL | NF-kB

CARMA1 (also known as CARD11 or Bimp3), B-cell lymphoma-10 (BCL10) and Mucosa-associated-lymphoid-tissue lymphoma-translocation gene 1 (MALT1) have an essential role in antigen receptor-induced nuclear factor-κB (NF-κB) activation and the control of lymphocyte activation and proliferation (1, 2). It is thought that antigen receptor triggering leads to the formation of an oligomeric CARMA1-BCL10-MALT1 complex that subsequently activates downstream elements of the NF-κB pathway (1, 3). MALT1 plays a key role in this process; it acts both as a scaffold to recruit additional signal transducers and as an enzyme with proteolytic activity that cleaves signaling proteins to favor T-cell activation (4). Recently, a tumor-promoting role for MALT1 has been proposed in diffuse large B-cell lymphoma (DLBCL) (5), the most common form of non-Hodgkin's lymphoma, comprising 30–40% of identified cases. At least three subtypes of DLBCL have been described based on differences in the underlying transforming mechanisms: germinal center B cell-like (GCB) DLBCL, activated B cell-like (ABC) DLBCL, and primary mediastinal B-cell lymphoma (PMBL). ABC DLBCL is characterized by constitutive NF-κB activation via the CARMA1/BCL10/MALT1 signaling pathway (5–8). The identification of oncogenic CARMA1 mutations in human DLBCL has identified CARMA1 as a bona fide oncogene (8). Oncogenic forms of CARMA1 showed constitutive oligomerization and an increased capacity to activate the NF-κB signaling pathway (8), but it has remained obscure how these oncogenic CARMA1 mutants affect signaling via the downstream components BCL10 and MALT1. We and others have recently identified a protease activity for MALT1 that is induced upon TCR triggering and required for optimal TCR-induced NF-κB activation (9, 10). However, it has remained unclear whether the MALT1 protease activity is indeed relevant for lymphocyte proliferation, and whether inhibition of the protease activity of MALT1 might be a useful strategy to therapeutically target DLBCL.

Results

We first assessed the activity of MALT1 in established DLBCL cell lines by monitoring the cleavage status of the MALT1 substrate BCL10 (10). Cells were stimulated with PMA and ionomycin, a combination of drugs that mimics many aspects of antigen receptor-induced lymphocyte activation, and analyzed by Western blot using an antibody directed against BCL10 or an antibody specifically detecting cleaved BCL10, which served as readout for MALT1 activity (Fig. 1 and Fig. S1). Constitutive BCL10 cleavage was detected in the ABC DLBCL cell lines OCI-Ly3, OCI-Ly10, HBL-1, and U2932, but not in the GCB DLBCL cell lines BJAB, SUDHL-4, and SUDHL-6 nor in the PMBL lines U2940, Karpas1106, and MedB1, which either showed inducible or no BCL10 cleavage (Fig. 1*A*). We did observe BCL10 cleavage in primary patient samples of DLBCL (Fig. S2). However, BCL10 cleavage was seen in both ABC and GCB DLBCLs, suggesting that activated T cells in the biopsy specimens may contribute to this cleavage.

We next treated DLBCL cell lines with z-VRPR-fmk, a cell-permeable and irreversible MALT1 inhibitor (10), and assessed its effect on BCL10 cleavage. Upon treatment of the cells with z-VRPR-fmk for 3 days or longer, only uncleaved BCL10 remained detectable in the ABC DLBCL cell lines OCI-Ly3 and OCI-Ly10, suggesting that the inhibitor had efficiently blocked the proteolytic activity of MALT1 (Fig. 1*B*). Recently, the NF-κB inhibitor A20 has been identified as a substrate of MALT1 which might be responsible for the NF-κB-promoting proteolytic activity of MALT1 (9). Therefore, expression and cleavage of A20 was assessed by Western blot in various DLBCL lines pretreated with or without the MALT1 inhibitor for 36 h. In contrast to DLBCL of the GCB subtype, ABC DLBCL cells showed higher expression and constitutive cleavage of A20 into multiple fragments, which could be inhibited by treatment of the cells with the MALT1 inhibitor (Fig. 1*C* and Fig. S3). Next, we tested whether oncogenic CARMA1 mutants previously identified from biopsies of human DLBCL (8) were able to induce MALT1 activity upon transfection into the GCB DLBCL cell line BJAB. Under these conditions, the two different oncogenic forms of CARMA1 were clearly more potent than wild-type CARMA1 in inducing cleavage of the MALT1 substrates BCL10 and A20 in the absence of an antigenic stimulation (Fig. 1*D*). Thus, constitutive MALT1

Author contributions: S.H., G.L., V.N., A.P.-F., L.M.S., and M.T. designed research; S.H., G.L., V.N., A.P.-F., and M.G. performed research; F.R., E.-M.M.P., J.D., W.C.C., and L.M.S. contributed new reagents/analytic tools; S.H., G.L., V.N.N., A.P.-F., L.M.S., and M.T. analyzed data; and S.H. and M.T. wrote the paper.

The authors declare no conflict of interest.

This article is a PNAS Direct Submission.

[1]Present address: Charité–Humboldt University, Campus Virchow, Department of Hematology/Oncology, Berlin, Germany.

[2]To whom correspondence should be addressed. E-mail: margot.thomeMiazza@unil.ch.

This article contains supporting information online at www.pnas.org/cgi/content/full/0907511106/DCSupplemental.

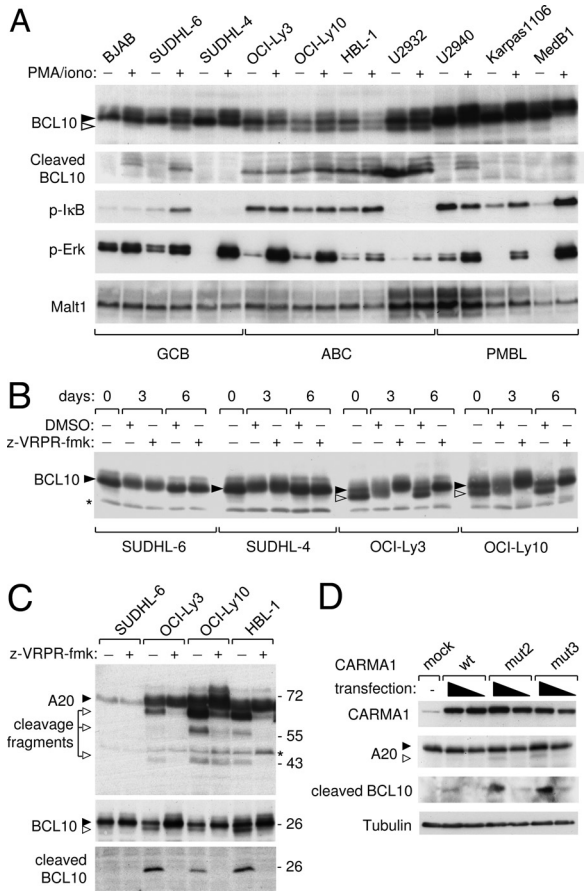

Fig. 1. Constitutive MALT1 activity in ABC-DLBCL. (*A*) Indicated cell lines were incubated for 30 min in the presence or absence of PMA and ionomycin, and postnuclear lysates were analyzed by Western blotting for the presence of total and cleaved BCL10, MALT1 and phosphorylated (activated) forms of ERK and IκB. Data are representative of at least three independent experiments. (*B*) Indicated cell lines were treated for the indicated times with the MALT1 inhibitor z-VRPR-fmk or solvent (DMSO), and postnuclear lysates were analyzed by Western blotting for the presence of BCL10 and its cleaved isoform. Black and white arrowheads indicate migration of non-cleaved and cleaved BCL10, respectively. A non-specific cross-reactive band detected by the anti-BCL10 antibody is indicated by an asterix (*). Data are representative of at least three independent experiments. (*C*) The indicated DLBCL lines were either left untreated or treated for 36 h with the MALT1 inhibitor z-VRPR-fmk or solvent (DMSO), and postnuclear lysates were analyzed by Western blotting as indicated. Black arrowheads indicate uncleaved, white arrowheads indicate cleaved forms of A20 or BCL10. A non-specific cross-reactive band detected by the anti-A20 antibody is indicated by an asterix (*). Data are representative of two independent experiments. (*D*) Activation of MALT1 by oncogenic CARMA1 mutants was assessed by co-transfection of indicated CARMA1 expression constructs or mock plasmid into BJAB cells, and analysis of BCL10 and A20 cleavage by Western blot. Loading was controlled by blotting for tubulin. Data are representative of two independent experiments.

activation is a consistent feature of ABC-DLBCL that can result from oncogenic CARMA1 mutations.

We and others have recently shown that the proteolytic activity of MALT1 is important for optimal NF-κB activation in antigen receptor-stimulated lymphocytes (9, 10). Therefore, we next assessed the relevance of the MALT1 protease activity for the expression of NF-κB-regulated genes. To this purpose, the ABC DLBCL lines HBL-1 and OCI-Ly3 were treated for increasing times with the MALT1 inhibitor z-VRPR-fmk, and relative changes in gene expression were assessed by whole genome gene expression arrays (Fig. 2). An NF-κB target gene signature (see *Materials and Methods*) was subsequently applied to the gene expression data following inhibition with z-VRPR-fmk in HBL-1 and OCI-Ly3 cells. Treatment with the MALT1 inhibitor showed a significant reduction in the NF-κB target gene signature in both ABC DLBCL lines tested (Fig. 2), clearly indicating that inhibition of the protease activity of MALT1 results in suppression of the NF-κB pathway.

NF-κB activation can contribute to cellular transformation by inducing the expression of a set of anti-apoptotic proteins (11, 12). To test whether the expression of anti-apoptotic proteins was altered in ABC DLBCL, we first assessed the expression of Bcl-XL and A1, two anti-apoptotic Bcl-2 protein family members whose gene expression is known to be controlled by NF-κB (13–15). ABC DLBCL but not GCB DLBCL cells showed high constitutive expression of Bcl-X and A1, and expression of both proteins was reduced upon treatment of the cells with the MALT1 inhibitor (Fig. 3*A*). We next tested the expression of the caspase-8 inhibitor FLIP, which is regulated by NF-κB (16, 17). In contrast to GCB DLBCL, ABC DLBCL expressed high constitutive levels of both the long and short splice isoforms of FLIP (FLIP-L and FLIP-S) (Fig. S4). Treatment of ABC DLBCL lines with z-VRPR-fmk indeed led to reduced expression of FLIP, which was most prominent for FLIP-S, which has a shorter protein half life than FLIP-L (18) (Fig. 3*B*). Consistent with these results, downregulation of the genes encoding A1 and FLIP was also observed in the gene array experiments (Fig. 2, genes BCL2A1 and CFLAR).

In addition to controlling the expression of anti-apoptotic proteins, NF-κB plays an important role for the expression of cytokines that are known to be essential for B-cell growth and survival (7, 12). Different ABC DLBCL tumors have been shown to express distinct but overlapping profiles of cytokines, most likely reflecting synergistic activity of NF-κB with other transcription factors such as STAT3 that is constitutively activated in some ABC DLBCL (19). Expression of the growth-promoting cytokine IL-6, for example, is coordinatively regulated by STAT3 and NF-κB at the transcriptional level, and is therefore secreted in high concentrations by OCI-Ly3 cells, which belong to the recently described STAT3-high subtype of ABC DLBCL (19). In these cells, the MALT1 inhibitor showed a strong reduction in the production of IL-6 (Fig. 3*C*). A similar reduction was observed in three other, STAT3-high ABC DLBCL lines that constitutively secrete IL-6 (Fig. 3*C*). Treatment with z-VRPR-fmk for 36 hours and more also led to a predominant reduction in the transcription and expression of IL-10 (Fig. 3*D*), which can promote the growth of activated B cells and B-cell lymphomas (20–22). The observed reduction of IL-6 and IL-10 cytokine levels in VRPR-fmk treated ABC DLBCL lines correlated with a decrease in the expression of these genes in two ABC DLBCL lines treated with the MALT1 inhibitor (Fig. 2). Moreover, it correlated with a clear decrease in the cellular levels of both total and phosphorylated STAT3 (Fig. 3*E*), most likely as a consequence of reduced cytokine receptor-induced signals that control the JAK2-dependent phosphorylation of STAT3 and the subsequent P-STAT3- and NF-κB-dependent feed-forward control of STAT3 gene expression in these cells (19).

Our data suggested that in ABC DLBCL, inhibition of MALT1 protease activity reduced expression of multiple NF-κB targets relevant for cellular proliferation and survival. We therefore tested whether inhibition of MALT1 affected viability, apoptosis frequency and cell cycle profile of DLBCL cell lines. Treatment of ABC DLBCL cells with 50 μM z-VRPR-fmk for 7 days drastically reduced the viability of the cells, while it did not affect viability of GCB DLBCL cells, even at considerably higher concentrations (Fig. 4*A* and Figs. S5 and S6). The effect on ABC DLBCL cells was not due to off-target effects of the inhibitor, since a strong reduction of cell viability was also observed when ABC DLBCL lines were transduced with a catalytically inactive form of MALT1 (C464A) that impairs its proteolytic activity

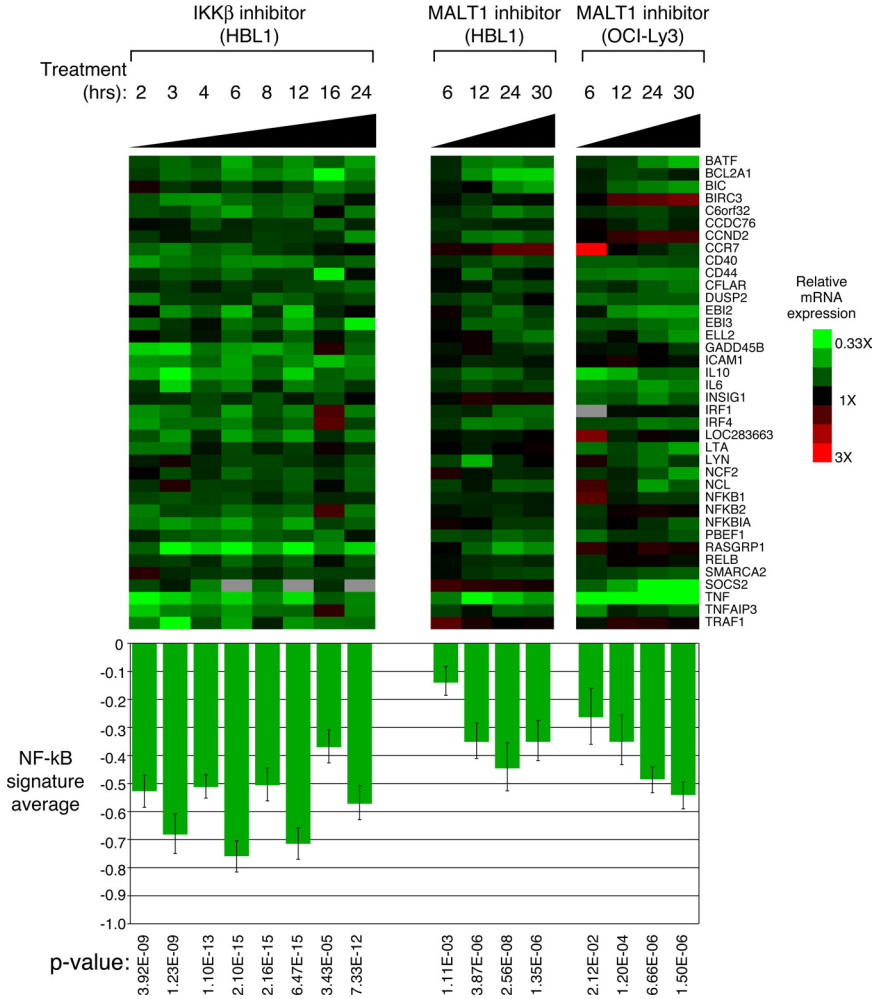

Fig. 2. Effect of MALT1 inhibitor treatment on NF-κB signature expression. The figure depicts gene expression profiling measurements (using Agilent oligonucleotide microarrays) from the HBL1 ABC DLBCL cell line treated with an IKKβ inhibitor (MLN120B, 25 μM) for the indicated times, according to the color scale at the right (gray color indicates that the spot did not meet data selection criteria). Shown are genes from a previously developed NF-κB target gene signature, which includes genes that were downregulated in expression following treatment of the ABC DLBCL cell lines OCI-Ly3 and OCI-Ly10 with the IKKβ inhibitor MLN120B or MLX105 (an older version of the same class of inhibitor) as measured on Lymphochip cDNA microarrays (NFκB_all_OCILy3_Ly10 signature (http://lymphochip.nih.gov/cgi-bin/signaturedb/signatureDB_DisplayGenes.cgi?signatureID = 83) (19, 34, 35). The figure depicts those NF-κB signature genes that were significantly downregulated in the IKKβ inhibitor treated HBL1 cells ($P < 0.02$ (paired *t*-test); 38/68 genes). Also shown are the expression levels of these NF-κB signature genes in HBL1 and OCI-Ly3 cells treated with the MALT1 inhibitor (z-VRPR-fmk, 50 μM). The NF-κB target genes were averaged for each sample and graphed at the bottom (error bars depict standard error of the mean). The significance of the decrease in the NF-κB signature average in each treated sample is also shown (paired *t*-test).

(Fig. 4*B*). Moreover, treatment with z-VRPR-fmk did not affect caspase-dependent or proteasome-dependent proteolytic activities that are relevant for some aspects of T-cell activation (Fig. S7). Treatment with the inhibitor or transduction with inactive MALT1 caused a clear increase in apoptotic cells (Fig. 4 *C* and *D*). Reduction in viability was dose-dependent in three independent ABC DLBCL tested, without notable cytotoxicity on GCB DLBCL at all concentrations tested (Fig. S5). Time course experiments showed that cell death became obvious after 3 days of treatment with z-VRPR-fmk and reached a maximal level after 5 days of treatment (Fig. S6). No such effects were observed with GBC DLBCL cell lines or an EBV-transformed ($LMP1^+$) Burkitt's lymphoma cell line (Raji) (Fig. 4 *A–D* and Figs. S5 and S6), which do not show constitutive MALT1 activity (Fig. 1). Finally, we also assessed the effect of MALT1 inhibition on the cell cycle profile of DLBCL lines. In the ABC DLBCL lines OCI-Ly3 and OCI-Ly10, cells treated with z-VRPR-fmk showed a significantly decreased ratio of cells in G2/M phase and an increased ratio of cells in subG0 phase compared to cells treated with DMSO alone, indicating reduced cellular division and increased cell death. In contrast, the inhibitor did not significantly affect the cell cycle profile of the GCB DLBCL lines SUDHL-4 and SUDHL-6, nor of other B-cell lymphoma cell lines such as Raji and SSK41 (Fig. 4*E*). Collectively, these data suggest that ABC DLBCL are characterized by constitutive proteolytic activity of MALT1, and that inhibition of MALT1 activity impairs the growth of ABC DLBCL lines by reducing the NF-κB-dependent expression of genes responsible for cellular growth and survival.

Discussion

The current standard therapy for patients suffering from DLBCL is a cyclophosphamide/doxorubicine/vincristine/prednisone chemotherapy combined with Rituximab, which cures a majority of patients with DLBCL of the GCB subtype (23). The three year progression-free survival of patients with ABC DLBCL following this treatment is however still only 40%, stressing the need for discovery of treatment options for ABC DLBCL

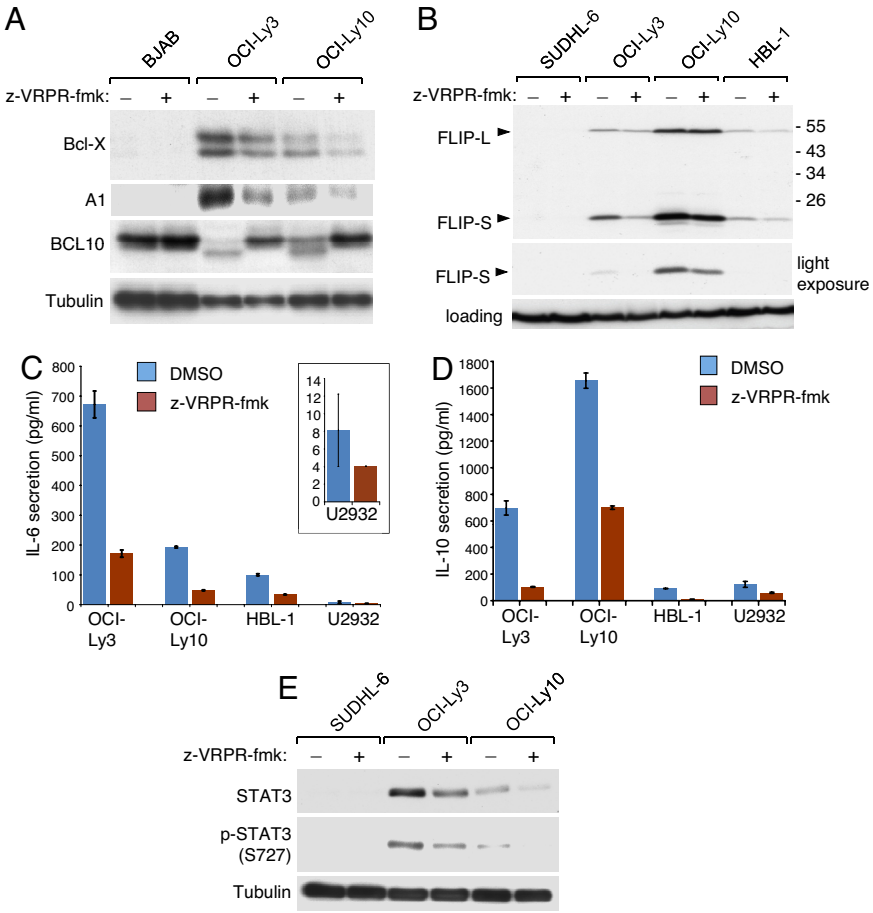

Fig. 3. Reduced expression of proliferation and survival proteins upon MALT1 inhibition. (*A* and *B*) The indicated GCB-DLBCL lines (BJAB, SUDHL-6) and ABC-DLBCL lines (OCI-Ly3, OCI-Ly10, HBL-1) were treated for 48 h with the MALT1 inhibitor z-VRPR-fmk or solvent (DMSO), and postnuclear lysates from equal cell numbers were analyzed by Western blotting for expression of apoptosis inhibitors Bcl-XL, A1 and FLIP and the presence of uncleaved (black arrowhead) or cleaved (open arrowhead) BCL10. Protein content of lysates was normalized by Bradford assay, and loading was controlled by blotting for tubulin. Data are representative of at least two independent experiments. (*C* and *D*) The indicated ABC-DLBCL lines were treated for 36 h with the MALT1 inhibitor z-VRPR-fmk or solvent (DMSO), and levels of IL-6 and IL-10 in the culture supernatant were assessed by ELISA. Data are expressed as mean of triplicate determinations ± SD and are representative of one to three independent experiments. (*E*) The GCB-DLBCL line SUDHL-6 and ABC-DLBCL lines OCI-Ly3 and OCI-Ly10 were treated for 48 h with the MALT1 inhibitor z-VRPR-fmk or solvent (DMSO), and postnuclear lysates were analyzed by Western blotting for expression and phosphorylation of STAT3. Loading was controlled by blotting for tubulin. Data are representative of at least two independent experiments.

(24). Constitutive activation of the CARMA1-BCL10-MALT1 signaling pathway was recently identified as a hallmark of these DLBCL (5, 8), but so far no suitable pharmacological strategy has been available to selectively inhibit this pathway. Here, we have identified and validated the proteolytic activity of MALT1 as a functionally critical element for the growth of ABC DLBCL, and identified MALT1 as a molecular target for the therapeutic attack of this cancer. Inhibition of MALT1 with an irreversible peptide-based inhibitor, z-VRPR-fmk, or by expression of a catalytically inactive form of MALT1, dramatically reduced the viability of cell lines derived from ABC DLBCL, but not from GCB DLBCL (Fig. 4 and Fig. S5). MALT1 inhibition correlated with decreased expression of genes such as FLIP (CFLAR), A1 (BCL2A1), A20 (TNFAIP3), IL-6, and IL-10 that are upregulated in primary tumors of ABC DLBCL (Fig. S8) and sensitive to NF-κB inhibition (19) (Fig. 2). Moreover, MALT1 inhibition led to reduced total and phosphorylated STAT3 levels, a hallmark of a recently described subset of primary human ABC DLBCL (19). Thus, our data obtained with DLBCL cell lines suggest that ABC DLBCL, and in particular the recently described STAT3-high subset of ABC DLBCL might respond to therapeutic attempts of MALT1 inhibition. Side effects of such a therapy are expected to be limited to immunosuppressive effects, since mice lacking MALT1 are perfectly viable and fertile, but show partially impaired adaptive and innate immune responses (25, 26). Importantly, MALT1-deficient mice can still eliminate herpesviral infections because of preserved cytolytic functions and proliferation of NK cells (27). It can be assumed that the immunosuppressive side effect of MALT1 inhibition in cancer patients would be milder than the immunodeficiency seen in MALT1-deficient mice, both because of the transient nature of chemotherapeutic treatments and because inhibition of the enzymatic activity of MALT1 would be expected to still preserve its essential scaffold functions (4). Therefore, the patients' capacity to respond to infections should be at least partially preserved in the face of treatment with a MALT1 inhibitor. Consistent with this idea is the fact that treatment of isolated primary human T cells and T-cell lines with saturating concentrations of the MALT1 inhibitor reproducibly led to partial (≈40–60%) inhibition of cytokine production (10). Proteases control many vital functions directly related to human health, and selective pharmacological inhibition of proteases has become a strategy for the rational therapy of diseases including cardiovascular disorders (28), neurodegeneration (29), osteoporosis, and bone metastasis (30) and viral infections (31). Interestingly, inhibitors of the proteasome have emerged as effective

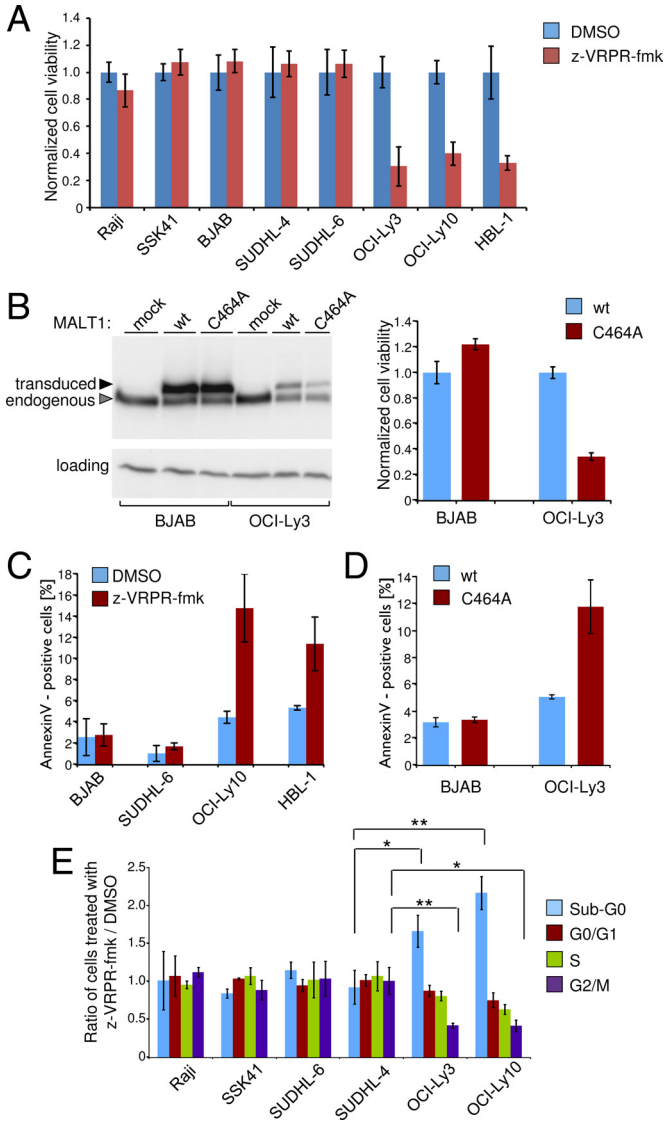

Fig. 4. Impaired survival and proliferation of ABC-DLBCL upon MALT1 inhibition. (*A*) Indicated DLBCL cell lines were either left untreated or treated for the indicated times with 50 μM of the MALT1 inhibitor z-VRPR-fmk or solvent (DMSO) for 7 days, and cell viability was tested using the MTT assay. Data are expressed as mean of triplicate determinations ± SD and are representative of three independent experiments. (*B*) Indicated cell lines were lentivirally transduced with expression vectors for wild-type (wt) or catalytically inactive (C464A) MALT1 or empty vector (mock). Cell viability was tested using the MTT assay 10 days after infection. Left panel shows expression levels of endogenous and transduced MALT1 and of Tubulin (loading) by Western blotting. Data are representative of three independent experiments. (*C* and *D*) Cells were treated as in (*A* and *B*), respectively, and apoptotic cells were quantified by flow cytometry, using AnnexinV staining. In (*D*), apoptotic cells were quantified 8 days after infection. Data are mean ± SD of two independent experiments. (*E*) Cells were treated as in (*A*) and cell cycle profiles were determined by flow cytometry using propidium iodide staining. The graph indicates the ratio of cells in the indicated stage of the cell cycle for DMSO versus inhibitor treated cells. Data are mean ± SD of two independent experiments. The statistical significance of the data were tested with an unpaired Student's *t*-test and the calculated goodness-of-fit value (*P* value) was determined (*, $P < 0.05$; **, $P < 0.01$).

drugs for the treatment of multiple myeloma and mantle cell lymphoma (32), and a recent study has shown that the proteasome inhibitor bortezomib enhances the activity of chemotherapy in relapsed or refractory forms of ABC but not GCB DLBCL (33). The therapeutic anti-tumor effect of proteasome inhibition is thought to be due, at least in part, to impaired proteasome-dependent degradation of the NF-κB inhibitor, IκB. However, this approach clearly has broad additional effects on the proteasome-dependent degradation of many other proteins, which can result in counterproductive and toxic side effects. Based on our identification of a crucial role for the MALT1 protease activity for the survival of ABC DLBCL, we propose the development of selective MALT1 inhibitors as a rational strategy for the therapy of this NF-κB-dependent type of cancer.

Materials and Methods

Antibodies. Primary antibodies used in this study included monoclonal mouse antibodies to phosphorylated Erk (MAPK-YT; Sigma), tubulin (B-5–1-2; Sigma), phosphorylated IκBα (5A5; Cell Signaling), A20 (59A426, eBioscience), Caspase-8 (MBL), rabbit anti-BCL10 (H-197 Santa Cruz Biotechnology), rabbit anti-active Caspase-3 (BD Biosciences), rabbit anti-PARP (Cell Signaling), monoclonal rabbit Bcl-XL (54H6, Cell Signaling), monoclonal rat anti-FLIP (Dave-2, Alexis Biochemicals) and affinity-purified rabbit anti-MALT1 generated against a GST-MALT1 fusion protein composed of amino acids 1–824 of human MALT1. For the generation of antibodies specific for cleaved BCL10, an octapeptide corresponding to the C terminus of cleaved BCL10 (MFLPLRSR) was coupled to KLH and used for immunization of rabbits (Eurogentec) and the obtained antiserum was affinity purified with the same peptide coupled to CNBr-activated Sepharose. The anti-A1 antibody was kindly provided by Dr. Bonnefoy-Berad (INSERM, Lyon, France). Horseradish peroxidase-coupled goat anti-mouse or anti-rabbit were from Jackson Immunoresearch.

Plasmids and Transfection of Cells. MALT1 wt and C464A expression constructs were generated as described (10). The MALT1 constructs were cloned into a lentiviral expression vector and cells were transduced as described (10). Expression constructs for wild-type CARMA1 and oncogenic CARMA1 mutants (mutant 2: L244P, derived from the ABC-DLBCL line OCI-Ly3, and mutant 3: G116S, derived from a lymphoma biopsy) have been described (8). For the expression of the CARMA1 constructs, 20×10^6 BJAB cells were resuspended in PBS supplemented with Ca^{2+}/Mg^{2+} (Gibco). Ten or thirty micrograms of wt or mutant CARMA1 expression construct or mock plasmid was added together with 5 μg of plasmid encoding SV40 Large T to the cell suspension, and cells were electroporated with the exponential protocol in BTX cuvettes with 4-mm gap size (Axonlab) at 230 V and 950 μF, using a Bio-Rad Gene Pulser Xcell. Transfected cells were cultured for 24 h before lysis.

Cells. The human lymphoma cells BJAB, SUDHL-4, SUDHL-6, HBL-1, OCI-Ly3, U2932, and U2940 were grown in RPMI medium 1640 supplemented with antibiotics and 10% FCS for BJAB and 20% FCS for the others. MedB1 and Karpas1106 were grown in Iscove's modified Dulbecco medium with antibiotics and 20% FCS. OCI-Ly10 were grown in Iscove's modified Dulbecco medium with antibiotics and 20% human serum (Blutspendezentrum Bern). The MedB1 cell line was kindly provided by Prof. Peter Möller (University of Ulm, Germany).

Cell Treatment and Lysis. B cell stimulation was initiated by the addition of PMA (10 ng/mL; Alexis) and ionomycin (1 μM; Calbiochem). Z-VRPR-fmk (Alexis Biochemicals) was dissolved in DMSO:H_2O (1:1) at 50 mM and added to lymphocytes at a final concentration of 50 μM, unless indicated otherwise. In some experiments, cells were treated with recombinant oligomeric FasL (2 μg/mL, Apotech) for 45 min or pretreated with 5 μM MG132 (Sigma Aldrich) for 30 min before stimulation. Cells were lysed in ice-cold HEPES-NaCl lysis buffer (50 mM HEPES, pH 7.4, 150 mM NaCl, and 1% Triton X-100) complemented with inhibitors of proteases (0.2 mg/mL AEBSF, 2 μg/mL aprotinin, and 10 μg/mL leupeptin) and phosphatases (50 mM NaF, 10 mM $Na_4P_2O_7$, and 10 mM $NaVO_4$). Postnuclear cell lysates were boiled with reducing SDS sample buffer and analyzed by SDS/PAGE. For optimal resolution samples were analyzed using Anderson gels as described (10).

Viability and Cell Proliferation Assays. For measuring cell viability, 5×10^4 cells were placed in a 96-well plate and incubated with the indicated treatments before determination of cell viability using MTT (Sigma, 500 μg/mL) or MTS (Promega, 400 μg/mL) and PMS (Sigma, 9 μg/mL), according to the manufacturer's instructions. Cell death was quantified by staining with FITC-coupled antibody to annexinV (Alexis Biochemicals). Cells (2×10^5) were incubated with a 1:20 dilution of the antibody in staining buffer (10 mM HEPES/NaOH, pH 7.4, 140 mM NaCl, and 2.5 mM $CaCl_2$) for 15 min at RT. Positive cells were

quantified by flow cytometry using a FACScan (BD). To calculate cell proliferation, 1×10^6 cells were permeabilized with 0.5% saponin, RNA was degraded by addition of 25 μg/mL RNase A (Roche) and DNA content was stained with 25 μg/mL PI (Fluka).

ELISA. Human IL-6 and IL-10 were quantified by ELISA (Immunotools) according to the manufacturer's instructions.

Gene Expression Profiling. RNA from HBL-1 cells was prepared 2, 3, 4, 6, 8, 12, 16, and 24 h following incubation with 25 μmol/L MLN120B (Millennium Pharmaceuticals) whereas RNA from HBL-1 and OCI-Ly3 cells was prepared 6, 12, 24, and 30 h following incubation with 50 mM z-VRPR-fmk. Total RNA was prepared using TRIzol reagent (Invitrogen) according to the manufacturer's recommendations. For each sample, 2 μg total RNA were used for the preparation of fluorescent probes. Gene expression was measured using whole-genome Agilent 4×44K gene expression arrays (Agilent), following the manufacturer's protocol. Signals from untreated HBL-1 or OCI-Ly3 cells (Cy3) were compared to respective MLN120B-treated or z-VRPR-fmk-treated cells (Cy5). A previously developed NF-κB target gene signature was applied to the gene expression data. This signature includes genes that were downregulated in expression following treatment of the ABC DLBCL cell lines OCI-Ly3 and OCI-Ly10 with the IKKβ inhibitor MLN120B or MLX105 (an older version of the same class of inhibitors), as measured on Lymphochip cDNA microarrays (NFκB_all_OCILy3_Ly10 signature (http://lymphochip.nih.gov/cgi-bin/signaturedb/signatureDB_DisplayGenes.cgi?signatureID = 83) (19, 34, 35).

ACKNOWLEDGMENTS. We thank Nicolas Fasel (Department of Biochemistry, University of Lausanne, Lausanne, Switzerland) and Nathalie Bonnefoy-Bérard (University of Lyon, Lyon, France) for reagents, Karen Leroy (Université Paris 12, Faculté de Médecine, Créteil, France) and Peter Möller (Abteilung für Pathologie des Universitätklinikums Ulm, Ulm, Germany) for cell lines, and members of the Thome laboratory for critical comments on the manuscript. This work was supported by grants from the Swiss National Science Foundation, the Swiss Cancer League, and the Pierre Mercier and Leenaards Foundations (to M.T.); the Intramural Research Program of the National Institutes of Health, National Cancer Institute, Center for Cancer Research; fellowships from the German Merit Foundation and the Faculty of Biology and Medicine of the University of Lausanne (to S.H.); and a research grant from the German Research Foundation (to G.L.). MLN120B was provided by Millennium Pharmaceuticals.

1. Rawlings DJ, Sommer K, Moreno-Garcia ME (2006) The CARMA1 signalosome links the signaling machinery of adaptive and innate immunity in lymphocytes. *Nat Rev Immunol* 6:799–812.
2. Thome M (2004) CARMA1, BCL-10 and MALT1 in lymphocyte development and activation. *Nat Rev Immunol* 4:348–359.
3. Schulze-Luehrmann J, Ghosh S (2006) Antigen-receptor signaling to nuclear factor kappa B. *Immunity* 25:701–715.
4. Thome M (2008) Multifunctional roles for MALT1 in T-cell activation. *Nat Rev Immunol* 8:495–500.
5. NgoVN, et al. (2006) A loss-of-function RNA interference screen for molecular targets in cancer. *Nature* 441:106–110.
6. Davis RE, Brown KD, Siebenlist U, Staudt LM (2001) Constitutive nuclear factor kappaB activity is required for survival of activated B cell-like diffuse large B cell lymphoma cells. *J Exp Med* 194:1861–1874.
7. Shaffer AL, Rosenwald A, Staudt LM (2002) Lymphoid malignancies: The dark side of B-cell differentiation. *Nat Rev Immunol* 2:920–932.
8. Lenz G, et al. (2008) Oncogenic CARD11 Mutations in Human Diffuse Large B Cell Lymphoma. *Science* 319:1676–1679.
9. Coornaert B, et al. (2008) T cell antigen receptor stimulation induces MALT1 paracaspase-mediated cleavage of the NF-kappaB inhibitor A20. *Nat Immunol* 9:263–271.
10. Rebeaud F, et al. (2008) The proteolytic activity of the paracaspase MALT1 is key in T cell activation. *Nat Immunol* 9:272–281.
11. Wang CY, Mayo MW, Korneluk RG, Goeddel DV, Baldwin AS, Jr (1998) NF-kappaB antiapoptosis: Induction of TRAF1 and TRAF2 and c-IAP1 and c-IAP2 to suppress caspase-8 activation. *Science* 281:1680–1683.
12. Karin M, Cao Y, Greten FR, Li ZW (2002) NF-kappaB in cancer: From innocent bystander to major culprit. *Nat Rev Cancer* 2:301–310.
13. Wang CY, Guttridge DC, Mayo MW, Baldwin AS, Jr (1999) NF-kappaB induces expression of the Bcl-2 homologue A1/Bfl-1 to preferentially suppress chemotherapy-induced apoptosis. *Mol Cell Biol* 19:5923–5929.
14. Lee HH, Dadgostar H, Cheng Q, Shu J, Cheng G (1999) NF-kappaB-mediated up-regulation of Bcl-x and Bfl-1/A1 is required for CD40 survival signaling in B lymphocytes. *Proc Natl Acad Sci USA* 96:9136–9141.
15. Tsukahara T, et al. (1999) Induction of Bcl-x(L) expression by human T-cell leukemia virus type 1 Tax through NF-kappaB in apoptosis-resistant T-cell transfectants with Tax. *J Virol* 73:7981–7987.
16. Micheau O, Lens S, Gaide O, Alevizopoulos K, Tschopp J (2001) NF-kappaB signals induce the expression of c-FLIP. *Mol Cell Biol* 21:5299–5305.
17. Kreuz S, Siegmund D, Scheurich P, Wajant H (2001) NF-kappaB inducers upregulate cFLIP, a cycloheximide-sensitive inhibitor of death receptor signaling. *Mol Cell Biol* 21:3964–3973.
18. Poukkula M, et al. (2005) Rapid turnover of c-FLIPshort is determined by its unique C-terminal tail. *J Biol Chem* 280:27345–27355.
19. Lam LT, et al. (2008) Cooperative signaling through the signal transducer and activator of transcription 3 and nuclear factor-{kappa}B pathways in subtypes of diffuse large B-cell lymphoma. *Blood* 111:3701–3713.
20. Voorzanger N, et al. (1996) Interleukin (IL)-10 and IL-6 are produced in vivo by non-Hodgkin's lymphoma cells and act as cooperative growth factors. *Cancer Res* 56:5499–5505.
21. Czarneski J, et al. (2004) Studies in NZB IL-10 knockout mice of the requirement of IL-10 for progression of B-cell lymphoma. *Leukemia* 18:597–606.
22. Rousset F, et al. (1992) Interleukin 10 is a potent growth and differentiation factor for activated human B lymphocytes. *Proc Natl Acad Sci USA* 89:1890–1893.
23. Staudt LM, Dave S (2005) The biology of human lymphoid malignancies revealed by gene expression profiling. *Adv Immunol* 87:163–208.
24. Lenz G, et al. (2008) Stromal gene signatures in large-B-cell lymphomas. *N Engl J Med* 359:2313–2323.
25. Ruland J, Duncan GS, Wakeham A, Mak TW (2003) Differential requirement for Malt1 in T and B cell antigen receptor signaling. *Immunity* 19:749–758.
26. Gross O, et al. (2006) Card9 controls a non-TLR signaling pathway for innate anti-fungal immunity. *Nature* 442:651–656.
27. Gross O, et al. (2008) Multiple ITAM-coupled NK cell receptors engage the Bcl10/Malt1 complex via Carma1 for NF-{kappa}B and MAPK activation to selectively control cytokine production. *Blood* 112:2421–2428.
28. Daull P, Jeng AY, Battistini B (2007) Towards triple vasopeptidase inhibitors for the treatment of cardiovascular diseases. *J Cardiovasc Pharmacol* 50:247–256.
29. Ghosh AK, Gemma S, Tang J (2008) beta-Secretase as a therapeutic target for Alzheimer's disease. *Neurotherapeutics* 5:399–408.
30. Le Gall C, Bonnelye E, Clezardin P (2008) Cathepsin K inhibitors as treatment of bone metastasis. *Curr Opin Support Palliat Care* 2:218–222.
31. Anderson J, Schiffer C, Lee SK, Swanstrom R (2009) Viral protease inhibitors. *Handb Exp Pharmacol* 189:85–110.
32. Nencioni A, Grunebach F, Patrone F, Ballestrero A, Brossart P (2007) Proteasome inhibitors: Antitumor effects and beyond. *Leukemia* 21:30–36.
33. Dunleavy K, et al. (2009) Differential efficacy of bortezomib plus chemotherapy within molecular subtypes of diffuse large B-cell lymphoma. *Blood* 113:6069–6076.
34. Lam LT, et al. (2005) Small molecule inhibitors of IkappaB kinase are selectively toxic for subgroups of diffuse large B-cell lymphoma defined by gene expression profiling. *Clin Cancer Res* 11:28–40.
35. Shaffer AL, et al. (2006) A library of gene expression signatures to illuminate normal and pathological lymphoid biology. *Immunol Rev* 210:67–85.